ON THE EFFECTS OF CLOCK OFFSET IN OFDM–BASED PASSIVE BISTATIC RADAR

Stephen Searle[⋆] *James Palmer*[†] *Linda Davis*[‡]

[⋆] Dept. of Elec. & Elec. Engineering, University of Melbourne
[†] Defence Science & Technology Organisation, Australia
[‡] Institute for Telecomms. Research, University of South Australia

ABSTRACT

In Passive Bistatic Radar (PBR) a local communications transmitter is used as an illuminator. A Line Of Sight (LOS) signal is captured to use as a template for radar processing. This may be cleaned via demodulation and remodulation, removing short–delay copies and sensor noise. However differences between the transmitter clock and local clock cause the remodulated signal to be mismatched to the transmitted signal, causing degradation of delay–Doppler processing output. This study presents a model which captures the effect of clock disparity upon remodulated OFDM signals. The model is used in simulation to illustrate the specific effect of clock offsets on PBR by examination of delay–Doppler output. It is shown that modification of the template to account for time–varying clock offsets can restore the delay–Doppler output to be nearly ideal.

Index Terms— Passive radar, OFDM, Signal reconstruction

1. INTRODUCTION

In Passive Bistatic Radar (PBR) an Illuminator Of Opportunity (IOO) such as a radio/TV transmitter is used in place of a dedicated radar transmitter. In recent years PBR has been attempted using analogue TV, FM radio, GSM, digital radio (DAB), digital terrestrial television (DVB–T), satellite and WiFi signals [1, 2]. Advantages of PBR include reduced hardware costs, the ability to operate covertly, a continuously operating transmitter, and the ability to use reserved bands of the spectrum for radar [3, 4, 5, 6].

Being reliant upon an IOO precludes any control over the transmitted signal [3]. A Line Of Sight (LOS) signal is obtained by direct observation of the signal from the transmitter for use as a template in radar processing. Such a signal is not perfect, possibly containing both measurement noise and short–delay copies of the transmission due to near clutter and multipath effects [7, 8, 6]. These artifacts can impair resolution and introduce false peaks in delay–Doppler output.

A template signal free of noise and clutter may be obtained by demodulating and then remodulating the LOS signal [7, 9, 8]. Also in the specific case of DVB–T, remodulation can mitigate inherent ambiguities due to signal structure by weighting pilot carriers [1, 10]. However due to disparity in clock rates of the transmitter and the receiver, a LOS signal remodulated with the local clock may not be adequately matched to the transmitted signal. This mismatch can cause significant leakage of power from returns and destroy resolution in delay–Doppler plots [3].

Recent studies using DVB–T for PBR estimated the disparity of transmitter and local clocks and incorporated this into the remodulated signal. Accounting for a constant offset improved the output of ambiguity processing, however some leakage from return lobes persisted and was deemed to be due to clock jitter. This was assumed to manifest as a phase coefficient which could be estimated at each OFDM symbol and introduced to the remodulated template [3, 10].

In this study we analyse an OFDM signal of the form specified by the DVB–T standard [11]. An expression for the received LOS signal is derived, making explicit the quantities which arise due to transmitter–receiver clock mismatch. The model is used to demonstrate that a realistic amount of clock jitter manifests as an approximately constant phase coefficient within each OFDM symbol, justifying the assumptions of [3, 10]. A simulated example illustrates the effect of demod/remod upon PBR performance, and demonstrates that range–Doppler output can be restored by incorporating correction phasors into the remodulated signal.

2. OFDM

Orthogonal Frequency Division Multiplexing (OFDM) is the underlying modulation in various communications signals, including DVB–T [11]. The bandwidth of the signal is small compared to the carrier (a factor of $\sim 10^2$ for DVB–T), but OFDM can be thought of as the simultaneous transmission of many narrowband signals, each transmitted at a slightly different carrier frequency and thus subject to different phase effects.

2.1. OFDM modulation

In the dth time period, an OFDM symbol is constructed by mapping a set of information–bearing QAM symbols $\{c_{dk}\}$ onto orthogonal carriers as follows:

$$x_d(t) = \frac{1}{N_u} \sum_{k=0}^{K} c_{dk} e^{i2\pi k/T_u (t-T_g)} \tag{1}$$

This is zero outside the domain $0 \leq t < T_f$. The first T_g seconds of this is redundant. The remaining T_u seconds is known as the useful part, so $T_f = T_u + T_g$, and is sampled with period T_s seconds to produce N_u samples, $N_f = N_u + N_g$. The full transmitted signal comprises individual OFDM symbols transmitted in sequence:

$$x(t) = \sum_{d=0}^{\infty} x_d(t - dT_f) \tag{2}$$

2.2. Effect of clock disparity in OFDM

Central to this study is the fact that the receiver in a PBR system has its own clock which may differ significantly from that of the transmitter. There may be a small difference in the base rates of the two clocks, and both clocks exhibit drift in clock rate over time, causing sampling jitter and phase noise. Without loss of generality it can be assumed that all clock–related imperfections can be mapped to one side [12]; we treat the receiver clock as being perfect and all clock imperfections manifesting on the transmitter side.

Sample Clock Error (SCO) causes issues when demodulating OFDM signals. Orthogonality between subcarriers may be lost, resulting in Inter–Carrier Interference (ICI). Cumulative clock jitter causes time drift and possibly Inter–Symbol Interference (ISI), and the phase of each carrier will be rotated [13, 14, 15, 16]. SCO is often modelled as a normalised offset in OFDM literature [16, 17, 13, 14]. Clock rate differences as high as 200 ppm have been considered though more typical values range from 10 to 100 ppm [14, 16, 17]. Clock jitter is related to oscillator phase noise [15, 18]. Jittered sample times may be modelled as a Wiener process, having the form:

$$t_n = nT + J_n \tag{3}$$

$$J_n = N(0, \sigma_N^2) + \alpha J_{n-1}, \quad 0 \leq \alpha \leq 1 \tag{4}$$

2.3. Time model used in this study

While the relative clock rate wanders over time, assume that during the dth OFDM symbol period the disparity between transmitter and receiver clocks is relatively constant. This disparity causes the apparent sampling rate of the transmitter to be T_d at the receiver. In this study the apparent time of the transmitter is modelled as an affine function of receiver time,

$$\tilde{t}_d(t) = \frac{T_d}{T_s} t + \rho_d, \qquad dT_f < t < (d+1)T_f \tag{5}$$

The time of the nth sample of the useful part of symbol d at the receiver, $t_d(n)$, is

$$t_d(n) = (n + \Delta_d)T_s \tag{6}$$

where $\Delta_d = dN_f + N_g$. At this time the apparent time of the transmitter, $\tilde{t}_d(n)$, is

$$\tilde{t}_d(n) = \frac{T_d}{T_s} t_d(n) + \rho_d, \qquad dT_f < t < (d+1)T_f \tag{7}$$

$$= T_d(n + \Delta_d) + \rho_d \tag{8}$$

where ρ_d chosen so $\tilde{t}$ is not discontinuous at symbol boundaries:

$$\tilde{t}_d(N_u) = \tilde{t}_{d+1}(-N_g) \tag{9}$$

$$\Rightarrow \ \rho_d = \rho_{d-1} + (T_{d-1} - T_d)dN_f \tag{10}$$

3. TRANSMISSION, RECEPTION AND DEMODULATION

3.1. Carrier modulation

A baseband OFDM signal is formed as in (2) and transmitted at carrier frequency f_c. The full OFDM signal at carrier is

$$x^c(t) = e^{i(\phi_c + 2\pi f_c t)} \sum_{d=0} x_d(t - dN_f T_s) \tag{11}$$

and the dth OFDM symbol at carrier:

$$x_d^c(t) = e^{i(\phi_c + 2\pi f_c (t + dN_f T_s))} x_d(t) \tag{12}$$

3.2. Received signal

The nth sample in block d is what the transmitter sent at $\tilde{t}_d(n)$. Note that transmission delay is accounted for in the receiver, when the signal is synchronised to the start of an OFDM symbol. We consider this absolute time to be the same in the transmitter and receiver and omit it from the model without penalty. What concerns us is the relative changes in time as clock sample rates change.

The received signal at carrier is

$$y_d^c(t) = y^c(t + dN_f T_s), \qquad 0 \leq t < T_f \tag{13}$$

$$= x^c(\tilde{t}_d(t + dN_f T_s)) \tag{14}$$

Note that in practice there will be some distortion of signal amplitude and phase due to channel effects. Clock disparity effects are not affected by the channel so we omit it from the model for simplicity.

The apparent carrier is estimated as $\hat{f}_{\text{app}}$ over all OFDM symbols in the Coherent Processing Interval (CPI) and this is used to demodulate the signal. For convenience define f'_d as:

$$f'_d = \frac{T_d}{T_s} f_c - \hat{f}_{\text{app}} \tag{15}$$

The downmixed signal is thus

$$y(t) = e^{-i2\pi \hat{f}_{\text{app}} t} y^c(t) \tag{16}$$

$$= e^{i\phi_c} e^{i2\pi f'_d t + f_c \rho_d} \sum_d x_d(\frac{T_d}{T_s} t + \rho_d - dNfT_s) \tag{17}$$

and the samples of the useful part of the dth symbol:

$$y_d[n] = y_d(nT_s + T_g) \tag{18}$$

$$= e^{i(\phi_c + 2\pi(f_c \rho_d + f'_d \Delta_d T_s))} e^{i2\pi f'_d T_s n} x_d[\tilde{n}_d(n)] \tag{19}$$

where $\tilde{n}_d$ is the equivalent sample index,

$$\tilde{n}_d = \left(\frac{T_d}{T_s} - 1\right)\Delta_d + \frac{T_d}{T_s} n + \frac{\rho_d}{T_s} \tag{20}$$

3.3. Discrete Fourier Coefficients

The useful samples of each symbol of the received signal (19) are Fourier transformed in order to recover the message symbols c_{dk}. Since $\left|\frac{T_d}{T_s} - 1\right|$ is small, then providing also that $f'_d T_u$ is small the influence of the ℓth carrier upon the kth Fourier bin, $\ell \neq k$, is not large. An approximate expression for the kth Fourier bin of the dth symbol which ignores ICI is thus

$$Y_d[k] = c_{dk} e^{i(\phi_c + 2\pi f_c \rho_d + 2\pi f'_d T_s \Lambda_d)} e^{i\frac{2\pi}{N_u} k((\frac{T_d}{T_s} - 1)\Lambda_d + \rho_d / T_s)} \tag{21}$$

where $\Lambda_d = \Delta_d + \frac{N_u - 1}{2}$.

4. REMODULATION

4.1. Naïve remodulation

The LOS signal is demodulated by extraction (and possibly correction) of the underlying QAM symbols c_{dk} in each OFDM symbol. Baseband remodulation can be done without regard to SCO by modulation of the recovered c_{dk} with the local clock. This is equivalent to application of (17) with $\hat{T}_d = T_s$ and $\hat{\rho}_d = 0$. This approach is typical in PBR literature, see *e.g.* [19]

The phase error $Z_d[k]$ between the remodulated signal and the received signal is

$$Z_d[k] = \frac{Y_d[k]}{\hat{Y}_d[k]} \tag{22}$$

$$= e^{i(\phi_c + (2\pi f_c(\rho_d + (T_d - T_s)\Lambda_d)))} e^{i2\pi \frac{k}{N_u T_s}(\rho_d + (T_d - T_s)\Lambda_d)} \tag{23}$$

4.2. Remodulation with consideration of SCO

Estimates of clock history $\hat{T}_d$ can be used to regenerate the transmitted signal. Assuming $\hat{c}_{dk} = c_{dk}$, phase error between the remodulated signal and received signal is

$$Z_d[k] = e^{i(\phi_c + 2\pi f_c(\varrho_d + \epsilon_d \Lambda_d))} e^{i2\pi k/(N_u T_s)(\varrho_d + \epsilon_d \Lambda_d)} \quad (24)$$

where $\varrho_d = \rho_d - \hat{\rho}_d$ and $\epsilon_d = T_d - \hat{T}_d$ are the estimation errors. The above expression comprises a constant factor with respect to subcarrier k and a factor having a linear dependence on k. The constant factor is more sensitive to errors in estimation since $f_c \gg 1/T_s$.

If the SCO between local and transmitter clocks is constant then the offset T_{SCO} can be estimated from the entire CPI. The remodulated signal in each OFDM symbol $z_d[n]$ is then generated by remodulating the $\hat{c}_{dk}$ according to (19), using $T_d = T_s + \hat{T}_{\text{SCO}}$.

If the SCO varies over time then T_d must be estimated at each symbol and the remodulated signal constructed from these, symbol by symbol. However if the SCO variation is not large then it may be treated as constant over a CPI and the signal remodulated as such, followed by post–processing to correct any residual phase at each OFDM symbol. If the estimation errors ϱ_d and ϵ_d are small then the phase error of the SCO–remodulated signal varies little with subcarrier and may be approximated as constant at each OFDM symbol.

Let the phase correction in the dth OFDM symbol be θ_d. If the remodulated signal with constant SCO is $z_d[n]$ then the post–processed signal is

$$\tilde{z}_d[n] = z_d[n] \times e^{i\theta_d} \quad (25)$$

The θ_d might be available from the OFDM demodulation process, however a simple approach taken in [3] was to compute the inner product of each remodulated symbol with the LOS symbol from which it was reconstructed:

$$\theta_d = \angle \sum_{n=0}^{N_u-1} y_d[n] z_d^*[n] \quad = \angle \sum_{k=0}^{K-1} Y_d[k] Z_d^*[k] \quad (26)$$

$$= \angle e^{i2\pi\epsilon_d f_c \Lambda_d} \sum_{k=0}^{K-1} c_{dk} \hat{c}_{dk}^* e^{i\frac{2\pi}{N_u T_s} k(\epsilon_d \Lambda_d + \varrho_d)} \quad (27)$$

The phasor inside the sum varies little, due to $\frac{\epsilon_d}{T_s} \ll 1$, and may be approximated with a constant $e^{i\gamma_d}$. Thus

$$\theta_d \approx 2\pi\epsilon_d f_c \Lambda_d + \gamma_d \quad (28)$$

5. SIMULATED EXAMPLE

5.1. Discrete–time radar ambiguity surfaces

One measure of a radar waveform's utility is its ambiguity surface [20]. The discrete–time cross–ambiguity function may be defined as

$$\chi_{xy}(\eta, \nu) = \left| \sum_{n=0}^{N_\chi - 1} y[n] x^*[n - \eta] e^{-i2\pi\nu n} \right| \quad (29)$$

where (η, ν) are the delay and Doppler variables respectively. The ambiguity surface of a DVB–T signal is almost ideal, having a peak at zero–delay and zero–Doppler, and a near–flat pedestal [1] (fig. 1).

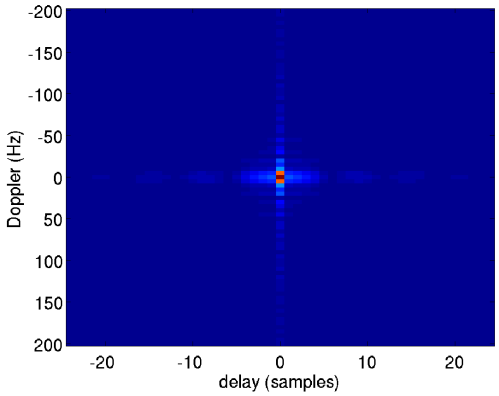

Fig. 1. Ambiguity of simulated signal

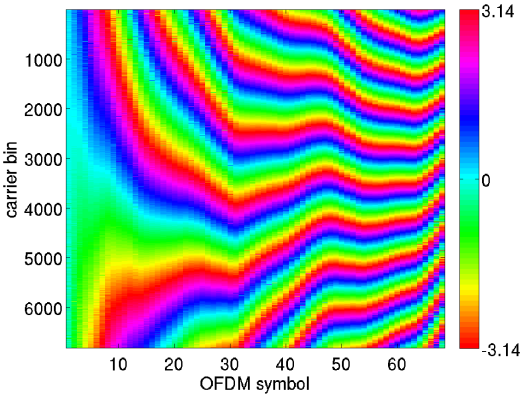

Fig. 2. SCO phasors obtained from simulated timeseries data.

5.2. Simulation

A clock–offset history over 68 symbols (1 DVB–T frame) is generated by the recursive application of (30) for a given initial offset τ_0 ppm and per–OFDM symbol deviation σ_τ ppm

$$\tau_{d+1} = \tau_d + \zeta_d \quad (30)$$

$$\zeta_d \sim N(0, \sigma_\tau^2) \quad (31)$$

This is converted to an apparent sample period history via

$$T_d = T_s \times (1 + \tau_d \times 10^{-6})^{-1} \quad (32)$$

One frame of random QAM symbols are generated and used with T_d to generate a timeseries signal via (17).

5.3. Example

A signal is generated as described above with values $\tau_0 = 20$ ppm and $\sigma_\tau = .04$ ppm. The phase distortions introduced by clock jitter are computed by Fourier transforming the useful component of each OFDM symbol, dividing each bin by the corresponding message symbol c_{dk} and taking complex angle. This is displayed in fig. 2. Note that the base phase at each symbol wanders as symbol index increases, and that the variation with Fourier bin also increases with symbol index.

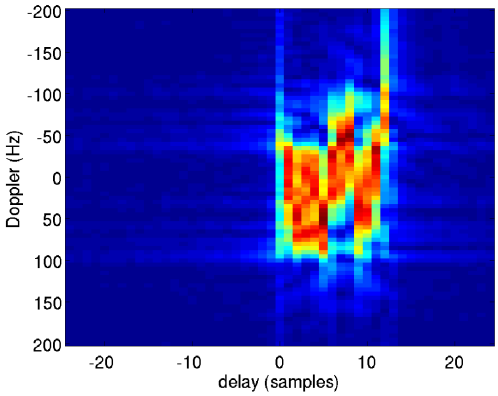

Fig. 3. Cross–ambiguity, simulated signal with naïve remodulation.

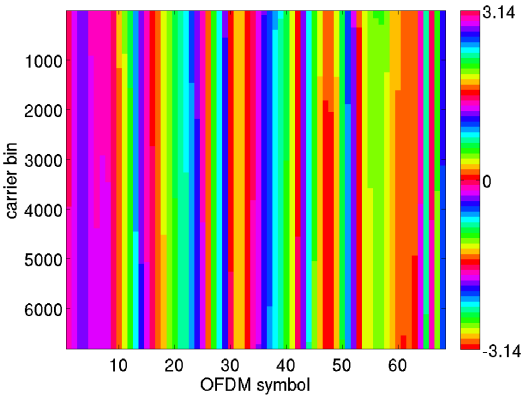

Fig. 4. Phase error in constant–SCO remod signal

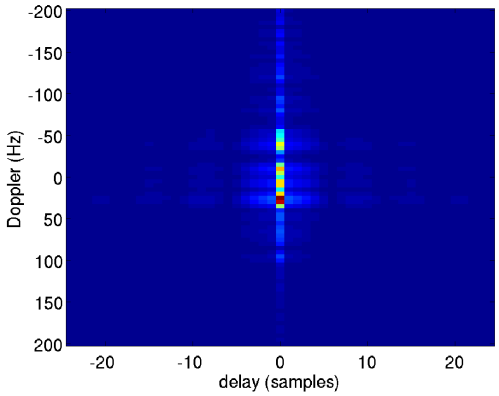

Fig. 5. Cross–ambiguity, simulation with constant–SCO remod

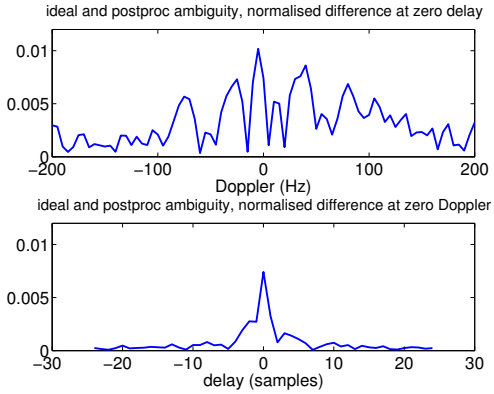

Fig. 6. Difference between ideal and postproc ambiguities

A naïvely remodulated signal is generated by modulating the same QAM data with the nominal sample clock period $T_d = T_s$. No noise is added to the simulated data and no errors introduced to the QAM symbols in order to examine the best case scenario; analysis of demodulation performance in noise is beyond the scope of this study. The cross–ambiguity surface of the simulated and naïvely remodulated signals is presented in fig. 3. We observe a significant leakage of power away from the mainlobe in both delay and Doppler.

A second remodulated signal is formed using a constant estimate of the average sample clock period across the processing interval. The estimate is taken as the average value of the T_d generated in simulation. This represents the best possible estimate of T_{SCO}. Converting to the frequency domain and computing phase differences between simulated and remodulated signal (fig. 4) it is evident that the phase difference varies only a small amount across subcarrier, while varying significantly across OFDM symbols. The cross–ambiguity of this constant–SCO remodulated signal and the simulated signal is shown in fig. 5. We observe that the ambiguity is well–localised in delay but not Doppler.

A third remodulated signal is formed by taking the constant–SCO remodulated signal and post–processing to correct phase on a symbol–by–symbol basis as described by (25)–(28). The resulting cross–ambiguity surface is omitted here for reasons of space, but is visually identical to fig. 1. The normalised difference from ideal ambiguity is shown in (fig. 6) to be 1% or less on either axis.

5.4. General observations made over many simulations

With naïve remodulation the spread of power in range and Doppler increases with both τ_0 and σ_τ. The location of the maximum in range exhibits a linear dependence upon τ_0. With constant–SCO remodulation the ambiguity maximises consistently in the zero–range bin, for any reasonable value of τ_0 and σ_τ. However leakage of power in Doppler, and the location of the maximum, increases as a function of σ_τ but not τ_0.

6. CONCLUSION

This study has considered the impact of SCO upon PBR with OFDM signals. An expression for a received signal incorporating the effect of SCO has been presented. Jittered SCO is shown to cause signal phase to vary between OFDM symbols. The phase of each subcarrier is affected differently, but this difference is small compared to the overall effect on phase. Failure to account for SCO in a remodulated LOS signal causes severe degradation of PBR delay–Doppler output. For typical values of clock offset and jitter, treating SCO as constant over a CPI and remodulating accordingly results in phase error being nearly constant over subcarriers at each OFDM symbol. Corresponding ambiguity surfaces resolve properly in range but not Doppler. Approximating the residual phase offsets at each OFDM symbol as constant over subcarrier and post–processing the remodulated signal restores near–ideal properties to the ambiguity surface.

7. REFERENCES

[1] H.A. Harms, L.M. Davis, and J.E. Palmer, "Understanding the signal structure in DVB–T signals for passive radar detection," in *IEEE Radar Conference*, May 2010, pp. 532–537.

[2] C. Bongioanni, F. Colone, D. Langellotti, P. Lombardo, and T. Bucciarelli, "A new approach for DVB–T cross–ambiguity function evaluation," in *Proc. 6th Euro. Radar Conf.*, Oct. 2009.

[3] S. Searle, S. Howard, and J. Palmer, "Remodulation of DVB–T signals for use in passive bistatic radar," in *44th Asilomar Conf. on Signals Systems and Computers*, Nov. 2010, pp. 1112–1116.

[4] R. Saini and M. Cherniakov, "DTV signal ambiguity function analysis for radar application," *IEE Proc. Radar Sonar Navig.*, vol. 152, no. 3, pp. 133–142, June 2005.

[5] D. Poullin, "Passive detection using digital broadcasters (DAB,DVB) with COFDM modulation," *IEE Proc. Radar Sonar Navig.*, vol. 152, no. 3, pp. 143–152, June 2005.

[6] H.D. Griffiths, "New directions in bistatic radar," in *IEEE Radar Conference*, 2008.

[7] M.K. Baczyk and M. Malanowski, "Reconstruction of the reference signal in DVB–T–based passive radar," *Intl. Journal of Electronics and Communications*, vol. 57, no. 1, pp. 43–48, 2011.

[8] J. Palmer, S. Palumbo, A. Summers, D. Merrett, and S. Howard, "DSTO's experimental geosynchronous satellite based PBR," in *Intl. Radar Conference*, Oct. 2009.

[9] D.W. O'Hagan, J. Kuschel, J. Heckenbach, M. Ummenhofer, and J Schell, "Signal reconstruction as an effective means of detecting targets in a DAB–based PBR," in *11th Intl. Radar Symposium*, June 2010.

[10] J.E. Palmer, H.A. Harms, S.J. Searle, and L.M. Davis, "DVB–T passive radar signal processing," *to appear in IEEE transactions on Signal Processing*, 2013.

[11] "Digital television – terrestrial broadcasting part 1: Characteristics of digital terrestrial television transmissions," Australian Standard AS4599.1–2007.

[12] D. Petrovic, W. Rave, and G. Fettweis, "Common phase error due to phase noise in OFDM – estimation and suppression," in *15th IEEE International Symposium on Personal, Indoor and Mobile Radio Communications*, Sept. 2004, vol. 3, pp. 1901–1905.

[13] K.H. Won, J.S. Han, and H-J Choi, "Sampling frequency offset estimation methods for DVB–T/H systems," *Journal of Networks*, vol. 5, no. 3, pp. 313–320, Mar. 2010.

[14] L-H. Wang and H-F. Chi, "A pilot–less sample–time synchronization algorithm for high–mobility DVB–T receiving," in *IEEE International Conference on Acoustics, Speech and Signal Processing*, May 2006, vol. 4.

[15] V. Syrjälä and M. Valkama, "Analysis and mitigation of phase noise and sampling jitter in OFDM radio receivers," *International Journal of Microwave and Wireless Technologies*, vol. 2, no. 2, pp. 193–202, Apr. 2010.

[16] H-S. Chen and Y. Lee, "Novel sampling clock offset estimation for DVB–T OFDM," in *IEEE 58th Vehicular Technology Conference*, 2003, vol. 4, pp. 2272–2276.

[17] L. Wang and D. Xu, "A new sampling clock synchronization method in OFDM system," in *5th International Conference on Wireless Communications, Networking and Mobile Computing*, 2009, pp. 1–4.

[18] G. Fettweis, M. Löhning, D. Petrovic, M. Windisch, P. Zillman, and W. Rave, "Dirty RF: A new paradigm," *International Journal of Wireless Information Networks*, vol. 14, no. 2, pp. 133–148, 2007.

[19] C.R. Berger, B. Demissie, J. Heckenbach, P. Willett, and S. Zhou, "Signal processing for passive radar using OFDM waveforms," *IEEE journal of Selected Topics In Signal Processing*, vol. 4, no. 1, pp. 226–238, Feb. 2010.

[20] P. M. Woodward, *Probability and Information Theory with Applications to Radar*, Artech House, Norwood, MA, 1980.